Journal of Alloys and Compounds 509 (2011) 6427–6432

Contents lists available at ScienceDirect

Journal of Alloys and Compounds

journal homepage: www.elsevier.com/locate/jallcom

Synthesis and electrochemical properties of $Li_4Ti_5O_{12}$

G.Q. Liu[a,*], L. Wen[b], G.Y. Liu[a,c], Q.Y. Wu[a], H.Z. Luo[d], B.Y. Ma[a], Y.W. Tian[a]

[a] School of Material and Metallurgy, Northeastern University, Shenyang 110004, China
[b] Chinese Acad Sci, Inst Met Res, Shenyang Natl Lab Mat Sci, Shenyang 110016, China
[c] College of Materials Science and Engineering, Jilin University; Changchun 130025, China
[d] The Council for Scientific and Industrial Research (CSIR) in South Africa, South Africa

ARTICLE INFO

Article history:
Received 18 January 2011
Received in revised form 7 March 2011
Accepted 9 March 2011
Available online 13 April 2011

Keywords:
Inorganic compounds
Chemical synthesis
Electrochemical measurements
Electrochemical properties

ABSTRACT

The spinel compound $Li_4Ti_5O_{12}$ was synthesized by a solid state method. In this synthesizing process, anatase TiO_2 and Li_2CO_3 were used as reactants. The influences of reaction temperature and calcination time on the properties of products were studied. When calcination temperature was 750 °C and calcination temperature was 24 h, the products exhibited good electrochemical properties. Its discharge capacity reached 160 mAh g^{-1} and its capacity retention was 97% at the 50th cycle when the current rate was 1 C. When current rate increased to 10 C, its first discharge capacity could reach 136 mAh g^{-1}, and its capacity retention was 85% at the 50th cycle.

1. Introduction

Although graphite has been used as anode since lithium ion batteries was invented, spinel $Li_4Ti_5O_{12}$ has many advantages over it. One of the unique properties of $Li_4Ti_5O_{12}$ is that it shows negligible lattice change during the intercalation of Li ions. There is no structural change (zero-strain insertion material) in the charge–discharge process. With the zero-strain and zero-volumetric change characteristics, the structural degradation is significantly reduced during cycling. Therefore, excellent cyclability can be expected for spinel $Li_4Ti_5O_{12}$ [1]. Another important property of $Li_4Ti_5O_{12}$ is that it has electrochemical stability window for most common electrolytes because it offers a stable operating voltage of approximately 1.5 V vs. lithium. The formation of a solid–electrolyte-interphase (SEI) layer is prohibited in this voltage [2–4]. So it is safe for $Li_4Ti_5O_{12}$ spinel to be used in power batteries of large applications such as HEV and EV.

The present shortcoming of $Li_4Ti_5O_{12}$ material is its low intrinsic electronic conductivity, which prevents its rate performances. The electrochemical properties of $Li_4Ti_5O_{12}$ are dependent on synthesizing methods to a great extent. In order to improve its electrochemical properties, sol–gel method and other synthesizing methods including hydrothermal method [5], spray pyrolysis method [6], solvothermal synthesis [7], spray pyrolysis [8], rheological phase method [9,10] and so on, have been proposed. Using these methods, small amount of product can be synthesized, but these methods are not suit for mass production. Solid state reaction is a commonly used method to prepare electrode materials for lithium ion batteries. It is simple and suitable for mass production. However, electrochemical performances of the $Li_4Ti_5O_{12}$ prepared by solid state method are usually not satisfactory. This is due to the inhomogeneity, large size and irregular morphology of products synthesized by solid state method [11].

In this study, the ball milling was employed in order to obtain product with small and well-distributed particle size when the synthesis temperature was 750 °C. The synthesis conditions such as reaction temperature and calcination time were studied, and the appropriate ones were drawn.

2. Experimental

2.1. Preparation of the $Li_4Ti_5O_{12}$

The stoichiometric amounts of Li_2CO_3 and anatase TiO_2 with a Li:Ti molar ratio of 0.82:1 were weighed separately. Then they were mixed by planetary ball milling with methanol medium. The rotating speed was 300 rpm min^{-1}. The dried and mixed reactant mixture was heated in a muffle furnace at 700, 750, 800 and 850 °C for some time in air. The products were then obtained.

2.2. Measurements

The phase identification of the prepared samples was carried out by X-ray diffraction (XRD) using a X-ray powder diffractometer (Rigaku Co. Ltd., Multiflex). X-ray profiles were measured between 10 and 80° (2θ angle) with a monochromatic Cu Kα radiation source. The morphologies of the products were examined with a scanning electron microscope (SEM, FEI NOVA NANOSEM430).

* Corresponding author. Tel.: +86 024 83673860; fax: +86 024 83687731.
E-mail address: liugq@smm.neu.edu.cn (G.Q. Liu).

0925-8388/$ – see front matter © 2011 Elsevier B.V. All rights reserved.
doi:10.1016/j.jallcom.2011.03.078

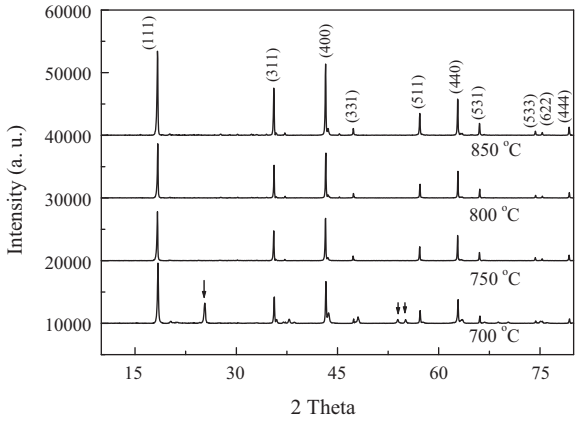

Fig. 1. XRD patterns of $Li_4Ti_5O_{12}$ samples synthesized at different temperatures for 16 h.

The electrochemical properties of products were tested in cells with metallic lithium as anode electrode. The cathode was separated from the Li anode by a layer of celgard 2300 membrane soaked with the electrolyte of 1 M $LiPF_6$ in a 1:1 (v/v) mixture of ethylene carbonate (EC) and dimethyl carbonate (DMC). The cathode was prepared by blade-coating a slurry of 80% (weight percent) active material, 10% conducting carbon black, and 10% PVDF binder in NMP on an aluminum foil, drying in an oven, roller-pressing and dried coated foil, and punching out circular discs of 1.23 cm^2. The cells were assembled into CR2025 coin cells in an argon-filled dry box. Charge–discharge tests were performed at a constant current density, in the range of 0.8–2.5 V. All the tests were carried out at room temperature.

Cyclic voltammetry (CV) was carried out at room temperature by using the above cells. CV was conducted at a scan rate of 0.1 mV s^{-1} between 0.8 V and 2.5 V versus Li/Li^+. In EIS measurement, the excitation voltage applied to the cells was 5 mV and the frequency range was between 100 kHz and 10 mHz.

3. Results and discussion

3.1. Phase and morphologies analysis of $Li_4Ti_5O_{12}$ samples synthesized at different temperatures

Fig. 1 shows the XRD patterns of the $Li_4Ti_5O_{12}$ samples synthesized at different temperatures. It is obvious that the sample synthesized at 700 °C is not a pure phase. The anatase TiO_2 component existed as the arrows directing. It is found that the diffraction patterns of all the specimens synthesized at above 800 °C are similar, with all the peaks indexable to the F_{d3m} space group. No obvious shift of the diffraction lines is found, which indicates comparable cell parameters of all the specimens, but small difference of the intensities of the peaks is found. In order to determine the lattice parameter, a, of the prepared samples, Bragg equation was used.

$$n\lambda = 2d_{hkl}\sin\theta$$

Here n is 1, λ is the wavelength of the incident X-ray beam which is 1.5406 Å, θ is the incident angle, and d_{hkl} is between the atomic layers of the cubic structure. Because the synthesized $Li_4Ti_5O_{12}$ is face centered cubic, the lattice parameter can be calculated by using the following equations:

$$d_{hkl} = \frac{a}{D}, \quad D = \text{square root of}(h^2 + k^2 + l^2)$$

where a is the lattice parameter and (hkl) are the Miller indices. The lattice parameters are obtained and listed in Table 1. It can be seen that the lattice parameters deceased slightly with increasing temperature. The reason is that the lithium can be lost due to volatilization at higher temperatures, resulting in lattice contraction. However, the lattice did not change significantly.

Table 1
The list of lattice parameter and volume at different synthesis temperatures.

Synthesis temperature, T (°C)	Lattice parameter, a (Å)	Volume, V (Å^3)
750	8.381	588.7
800	8.371	586.6
850	8.363	584.9

Fig. 2 shows the morphologies of the $Li_4Ti_5O_{12}$ particles synthesized at 750, 800 and 850 °C, respectively. We can see that the particles of $Li_4Ti_5O_{12}$ synthesized at 750 °C are well distributed. Most of them are around 0.5 μm, and small amount are larger than 0.5 μm. These particles exhibit polyhedral shapes. With synthesis temperatures increasing, the particle sizes become larger. This is because the secondary particles grow with increasing temperature.

3.2. Electrochemical properties

For solid state reactions, synthesis temperature is one of the important factors that affect the electrochemical properties of products. Electrochemical properties of products synthesized at different temperatures of 700, 750, 800 and 850 °C were investigated in this study. Fig. 3 shows the cycle performances at 0.2 C. The samples were synthesized at 700, 750, 800 and 850 °C for 16 h, respectively. All of the samples exhibited good cycle ability, but the discharge capacities of the samples were different. The sample synthesized at 750 °C delivered the highest capacity of 151 mAh g^{-1}. The discharge capacities are in a decreasing order for samples synthesized at 750, 800, 850 and 700 °C. That the sample synthesized at 700 °C delivered a low capacity is due to the existence of impurity. Although the samples synthesized at 750, 800 and 850 °C are pure phases, there are differences in particle size and diffraction peak intensity. The small particle size leads to reduced solid state diffusion length for lithium ions. So both the discharge capacity and capacity retention are excellent for the sample with small particle size.

Calcination time is another one of the important factors that affect the electrochemical properties of products. Here we investigated the electrochemical properties of products synthesized at 750 °C for 2, 8, 16, 24 and 32 h. The cycling stability of the samples is shown in Fig. 4. The sample sintered for 24 h exhibited the best electrochemical properties. At 0.2 C rate, it delivered a capacity of 160 mAh g^{-1} at the first cycle, and the capacity retention was 96.7% at the 50th cycle.

Fig. 5(a) shows the XRD patterns of $Li_4Ti_5O_{12}$ samples synthesized at 750 °C for different time. It indicates that there were impurities in product synthesized at 750 °C for 2 h. Its electrochemical properties deteriorated due to the impurities. The diffraction peaks began to shift towards small diffraction angle with increasing calcinations time from 8 to 32 h, as shown in Fig. 5(b). According to Bragg equation, if diffraction angle became smaller, the distance between atomic layers became larger. Larger distance between atomic layers was beneficial to migration of Li in structure. This is the reason that electrochemical properties of products improved with increasing calcinations time. However, the electrochemical properties of product did not continue to get better when calcinations time increased from 24 to 32 h. Fig. 6(a and b) shows the morphologies of $Li_4Ti_5O_{12}$ particles synthesized at 750 °C for 24 and 32 h, respectively. It can be seen that the particle size became larger when calcinations time increased from 24 to 32 h. The disadvantages of large particle include long path lengths for Li^+ transport, long path lengths for electronic transport, lower electrode/electrolyte contact area leading to lower charge/discharge rates. So the electrochemical properties of product synthesized at 750 °C for 24 h was better than the product synthesized at 750 °C for 32 h.

Figs. 7 and 8 show the charge–discharge results at different current rates of 0.2 C, 1 C, 5 C and 10 C. It can be seen that the capacities are almost the same when current rates are 0.2 C and 1 C. The cycling stability at 1 C was also as good as at 0.2 C. However, the

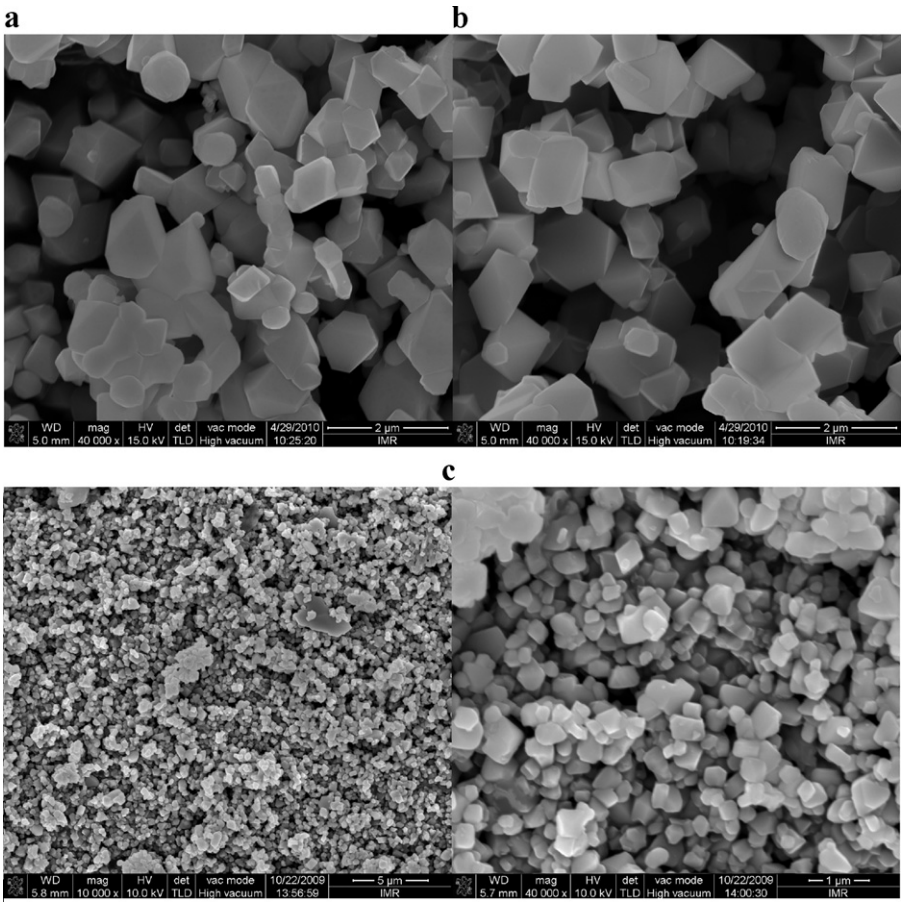

Fig. 2. Scanning electron micrograghs of $Li_4Ti_5O_{12}$ samples synthesized at 800 °C (a), 850 °C (b) and 750 °C (c) for 16 h.

discharge plateau at 0.2 C was higher than the discharge plateau at 1 C. With the current rate increasing to 5 C and 10 C, the capacities dropped to 134 and 126 mAh g^{-1} (5th cycle), respectively. The capacity retention was 96% at the 50th cycle at 5 C rate. At 10 C, the capacity decreased gradually with cycles proceeding. The capacity retention was 85% at the 50th cycle. These results are better than other solid state methods [12–14].

To further understand the kinetic behavior of electrode process, electrochemical impedance spectroscopy measurement was conducted. Fig. 9(a) shows the Nyquist plots of the $Li_4Ti_5O_{12}$ synthesized at 750 °C for 24 h in the open circuit state. The plots consist of a depressed semicircle in high-to-medium frequency range and a line inclined at constant angle to the real axis in low frequency range. The high-frequency intercept at the *x*-axis is typically attributed to the ohmic resistance of the cell (mainly contributed from the electrolyte), while the depressed semicircle in the high-to-medium frequency range is normally related to the complex reaction process over the electrolyte/electrode interface, which may also include the charge-transfer resistance

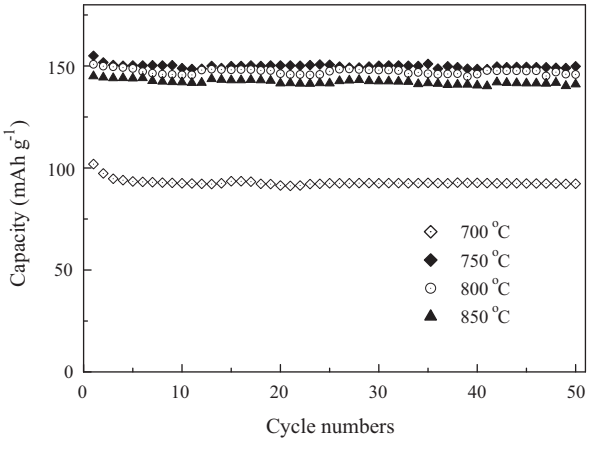

Fig. 3. Cycle performances of $Li_4Ti_5O_{12}$ samples prepared at different temperatures for 16 h.

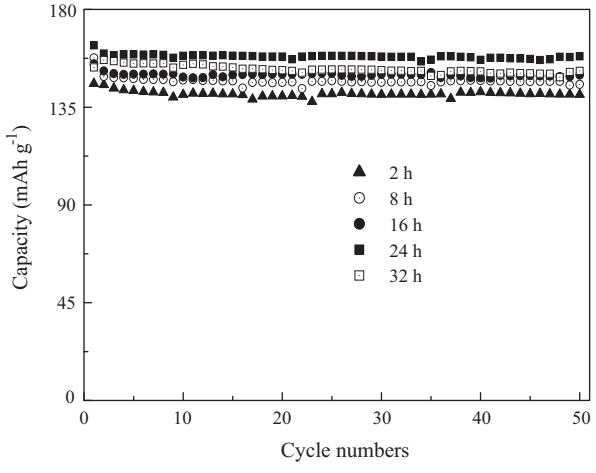

Fig. 4. Cycle performances of $Li_4Ti_5O_{12}$ samples prepared at 750 °C for different time.

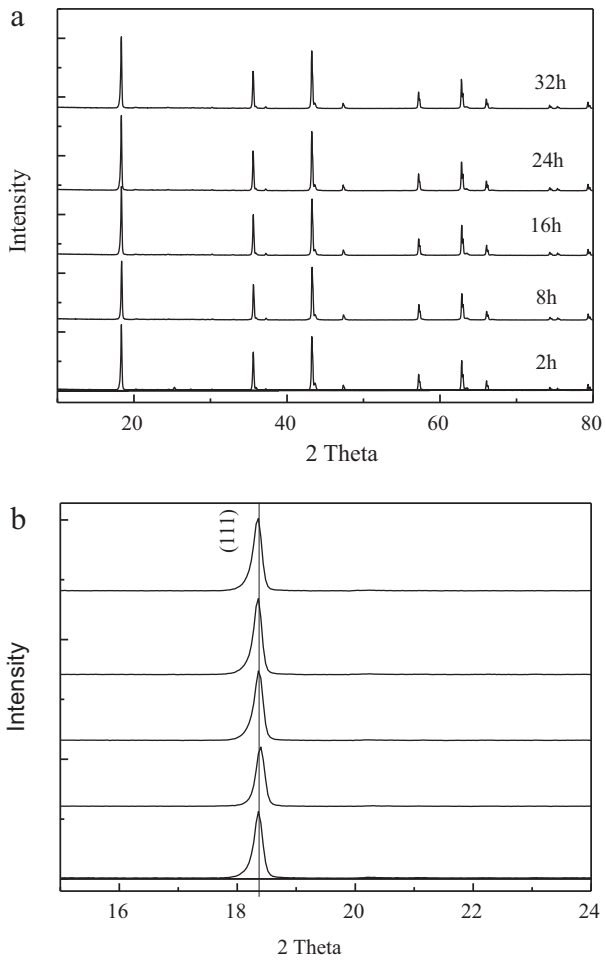

Fig. 5. (a) XRD patterns of $Li_4Ti_5O_{12}$ samples synthesized at 750 °C for different time. (b) The (1 1 1) peaks of XRD patterns of $Li_4Ti_5O_{12}$ samples.

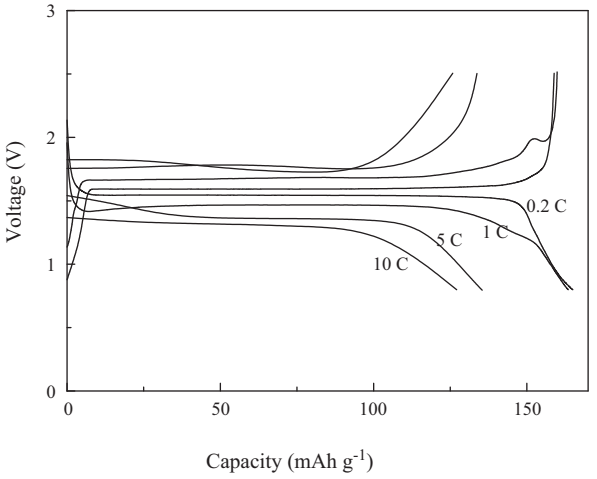

Fig. 7. Charge/discharge curves for $Li_4Ti_5O_{12}$ sample prepared at 750 °C for 24 h at 0.2 C, 1 C, 5 C and 10 C.

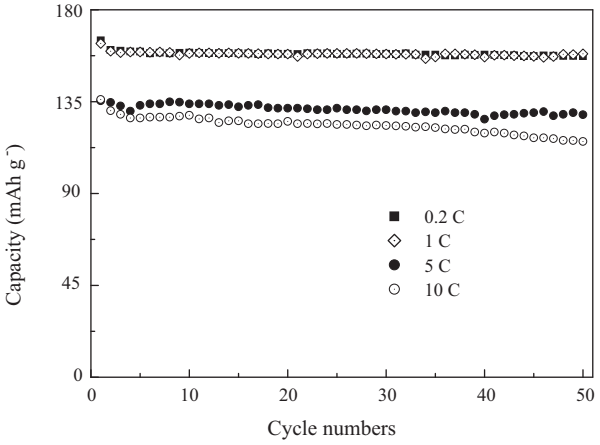

Fig. 8. Cycle performances of $Li_4Ti_5O_{12}$ sample prepared at 750 °C for 24 h at 0.2 C, 1 C, 5 C and 10 C.

and corresponding capacitances. The inclined line in the lower frequency range, attributed to the Warburg impedance, is associated with lithium-ion diffusion through the $Li_4Ti_5O_{12}$ electrode. The impedance spectrum is fitted by using the equivalent circuit as shown in Fig. 9(b). In the equivalent circuit, R_L indicates the ohmic resistance of electrolyte and electrode; R_{ct} is attributed to the charge transfer resistance at the active material interface; constant phase element Q1 represents the double-layer capacitance of the electrode–electrolyte interface. Z_w is the Warburg impedance caused by a semi-infinite diffusion of Li^+ ion in electrode and corresponds to the inclined line in the low frequency range. The fitted parameters of the equivalent circuit are given in Table 2. The dif-

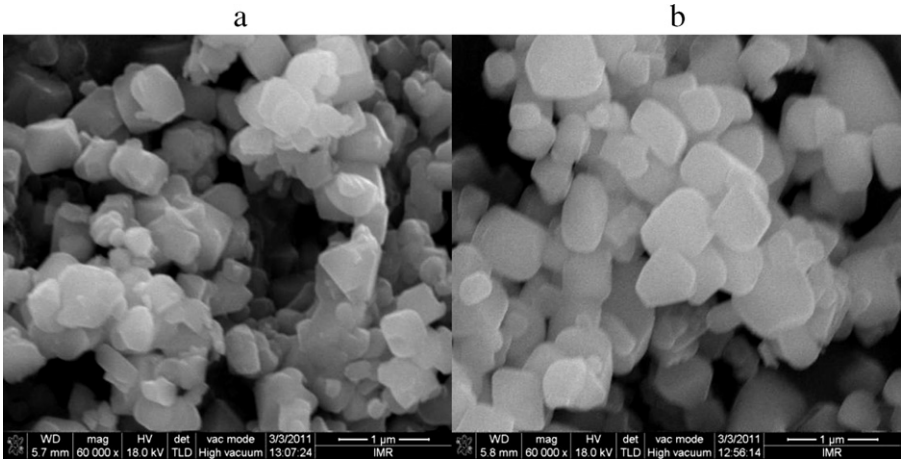

Fig. 6. Scanning electron micrograghs of $Li_4Ti_5O_{12}$ samples synthesized at 750 °C for 24 h (a) and 32 h (b).

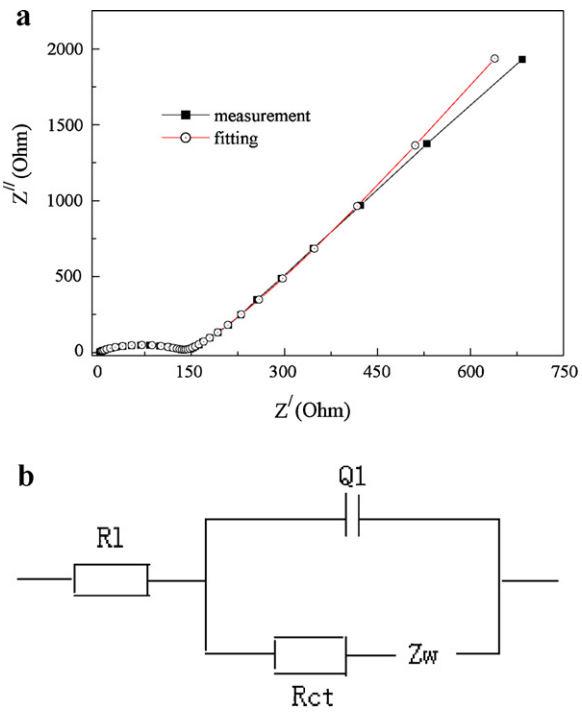

Fig. 9. (a) EIS Nyquist plots of experimental data and fitting results of $Li_4Ti_5O_{12}$, (b) equivalent circuit for EIS data fitting.

Table 2
EIS fitting results of $Li_4Ti_5O_{12}$.

Sample	R_L (ohm)	R_{ct} (ohm)	Q1 (F)	n_1	Z_w (ohm)
$Li_4Ti_5O_{12}$	1.848	133	1.676E-5	0.8016	0.1229

fusion coefficient of lithium ion can be calculated from the plots in the low-frequency region according to the following equations [15]:$D = \frac{R^2T^2}{2A^2n^4F^4C^2\sigma^2}$ and $Z_{re} = R_{ct} + R_L + \sigma\omega^{-1/2}$where R is the gas constant, T is the absolute temperature, n is the number of electron(s) per molecule oxidized, A is the surface area, F is Faraday's constant, C is the concentration of Li ions, D is the diffusion coefficient, σ is the Warburg factor, and ω is frequency.

Based on the experimental results, the relationship between Z_{re} and the reciprocal square root of ω in the low-frequency region can be obtained, as shown in Fig. 10. The σ value can be drawn as 64.38. Therefore, the diffusion coefficient of lithium ion is calculated to be around 1.1E−9 S cm^{-1}.

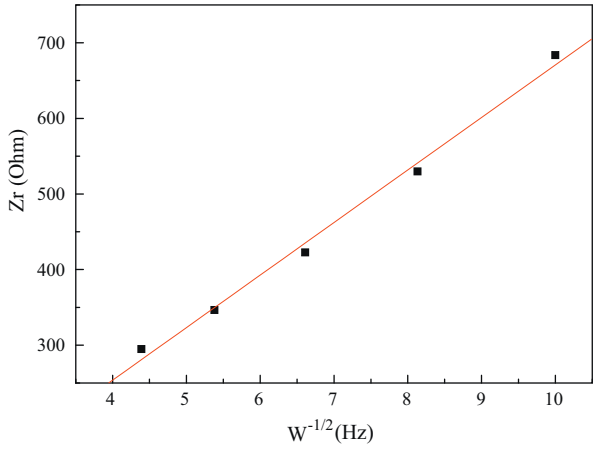

Fig. 10. Relationship between Z_{re} and $\omega^{-1/2}$ in the low-frequency region.

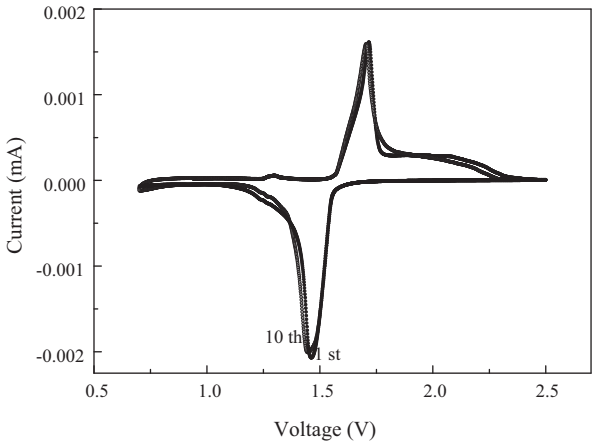

Fig. 11. Cyclic voltammogram of $Li_4Ti_5O_{12}$ sample prepared at 750 °C for 24 h.

Fig. 11 shows the cyclic voltammograms of $Li_4Ti_5O_{12}$ at the 1st and 10th cycle. One cathode peak that located at 1.46 V corresponds to the voltage flat of the discharge process. This is the process of Li insertion in spinel $Li_4Ti_5O_{12}$. Another anodic peak that located at 1.7 V corresponds to the voltage flat of the charge process. This is the process of Li deintercalation from spinel $Li_4Ti_5O_{12}$. The electrochemical reaction based on Ti^{4+}/Ti^{3+} redox couple is a reversible redox reaction. Furthermore, the 1st cyclic voltammogram almost matches together with the 10th cyclic voltammogram. It indicates that the $Li_4Ti_5O_{12}$ sample has good cycle performance. Another small anodic peak located at about 1.3 V was also observed. It cannot be attributed to an electrochemical process because a corresponding cathodic peak was not observed. Perhaps there are some problems when making the electrode, which results in this result.

4. Conclusion

In this study, spinel compound $Li_4Ti_5O_{12}$ was synthesized by a solid state method with ball milling process. The influences of reaction conditions such as reaction temperatures and reaction time on the products were investigated in detail. The product synthesized at 750 °C for 24 h exhibited small and well-distributed particle size. The charge–discharge and cyclic voltammogram tests demonstrated that it had good electrochemical properties. The discharge capacity reached 160 mAh g^{-1} and its capacity retention was 97% at the 50th cycle at 1 C. When current rate increased to 10 C, the first discharge capacity could reach 136 mAh g^{-1}, and the capacity retention was 85% at the 50th cycle. The diffusion coefficient of lithium ion was calculated as 1.1E−9 S cm^{-1} based on the EIS results.

Acknowledgement

This work was supported by the Study Abroad Funds of Northeastern University and China Postdoctoral Science Foundation Project (20100471467).

References

[1] T. Ohzuku, A. Ueda, J. Electrochem. Soc. 142 (1995) 1431.
[2] S. Zhang, M.S. Ding, K. Xu, J. Allen, T.R. Jow, Electrochem. Solid State Lett. 4 (2001) A206.
[3] E.P. Roth, D.H. Doughty, J. Franklin, J. Power Source 134 (2003) 224.
[4] J.S. Kim, S.W. Kim, H. Gwon, W.S. Yoon, K. Kang, Electrochim. Acta 54 (2009) 5914.
[5] J.R. Li, Z.L. Tang, Z.T. Zhang, Electrochem. Commun. 7 (2005) 894.
[6] S.H. Ju, Y.C. Kang, J. Phys. Chem. Solids 70 (2009) 40.

[7] Y. Li, H. Zhao, Z. Tian, W. Qiu, X. Li, J. Alloys Compd. 455 (2008) 471.
[8] S.H. Ju, Y.C. Kang, J. Power Source 189 (2009) 185.
[9] H. Liu, Y. Feng, K. Wang, J.Y. Xie, J. Phys. Chem. Solids 69 (2008) 2037.
[10] S.Y. Yin, L. Song, X.Y. Wang, M.F. Zhang, K.L. Zhang, Y.X. Zhang, Electrochim. Acta 54 (2009) 5629.
[11] Y. Hao, Q. Lai, Z. Xu, X. Liu, X. Ji, Solid State Ionics 176 (2005) 1201.
[12] G.F. Yan, H.H. Fang, H.J. Zhao, G.S. Li, Y. Yang, L.P. Li, J. Alloys Compd. 470 (2009) 544.
[13] X.L. Yao, S. Xie, C.H. Chen, Q.S. Wang, J.H. Sun, Y.L. Li, S.X. Lu, Electrochim. Acta 50 (2005) 4076.
[14] G.F. Yan, G.S. Li, L.P. Li, H.S. Fang, Chin. J. Struct. Chem. 28 (2009) 1393.
[15] A.J. Bard, L.R. Faulkner, Electrochemical Methods, Wiley, New York, 2001, p. 231.